


## Article

# A Cooperative Distributed Energy Management Strategy for Interconnected Microgrids Based on Model Predictive Control

Xiaolin Zhang <sup>1</sup>, Zhi Liu <sup>1,\*</sup>  and Chunyang Wang <sup>2</sup>

<sup>1</sup> School of Electronic Information Engineering, Changchun University of Science and Technology, Changchun 130022, China; hkc\_zxl@163.com

<sup>2</sup> Yahe School of Design and Engineering, Haikou University of Economics, Haikou 571127, China; jlpe\_wcy@163.com

\* Correspondence: liuzhi@cust.edu.cn

## Abstract

For interconnected multi-microgrids, it is crucial to improve operational economy and renewable energy utilization while ensuring system security. However, existing studies still face limitations in handling multi-time-scale uncertainties and enhancing the incentive for energy trading. Therefore, this paper proposes a cooperative distributed energy management strategy for interconnected microgrids based on model predictive control. First, a multi-time-scale framework is introduced into the multi-microgrid model, where rolling optimization and adaptive prediction/control horizons are used to cope with stochastic fluctuations of sources and loads. Then, a cooperative game model for the multi-microgrid coalition is formulated, and the asymmetric Nash bargaining problem is equivalently decomposed into a two-stage procedure of “coalition operation cost minimization–transaction bargaining”. Next, an algorithm for a distributed alternating-direction method of multipliers is employed for solution. Finally, multi-scenario simulations are carried out to compare three operation modes: independent operation, cooperation only, and model predictive control-based cooperation. The results show that compared with the independent operation mode, the total operation cost of the system is reduced by 22.8% using the proposed method and by 6.3% compared with the mode only adopting the cooperation mechanism, which demonstrates the effectiveness of the proposed strategy. The proposed strategy also enhances sustainability by improving local renewable energy accommodation, reducing reliance on upstream grid electricity, and supporting more resilient operation of interconnected microgrids under uncertainty.

**Keywords:** interconnected microgrids; model predictive control; cooperative game; energy complementarity; sustainable energy management



Academic Editor: Carlos Vargas-Salgado

Received: 24 January 2026

Revised: 23 February 2026

Accepted: 28 February 2026

Published: 3 March 2026

**Copyright:** © 2026 by the authors.

Licensee MDPI, Basel, Switzerland.

This article is an open access article distributed under the terms and conditions of the [Creative Commons Attribution \(CC BY\)](https://creativecommons.org/licenses/by/4.0/) license.

## 1. Introduction

With the rapid development of smart grids, microgrids (MGs) have gradually become key participants in future power-grid transactions [1,2]. The concept of a microgrid (MG) emerged in the context of the continuous aggregation of distributed energy resources. The operational capacity of a single MG is quite limited, and it is affected by changes in the operating environment, resulting in less-than-satisfactory anti-disturbance ability [3–5]. To coordinate various distributed energy resources and comprehensively consider operating costs and electricity demand, an MG energy management strategy is proposed [6,7]. The goal is to optimize the energy interaction and trading strategies between the MG cluster and

the main grid to enhance the stability, reliability, and energy efficiency of the power system. However, the inherent intermittency and volatility of renewable energy generation and the uncertainty of users' electricity demand still pose significant challenges with respect to energy management [8]. To address the above issues, this paper mainly focuses on research into two types of methods: model predictive control (MPC) and the cooperative game method.

Beyond economic dispatch, coordinated energy management of interconnected microgrids is also essential for sustainable energy development because it can improve local renewable energy utilization, reduce dependence on centralized fossil fuel-dominated grid supply, and enhance the resilience of regional energy systems under uncertainty.

MG clusters have different control architectures, such as centralized, decentralized, and distributed modes [9–11]. In centralized control architectures, the central controller uniformly coordinates the operation and energy interaction of each MG. However, there are issues with the safeguarding of data privacy of individual MGs, and when the cluster scale expands, the problem of increased computational pressure is introduced [12]. In the decentralized control mode, each MG can make independent decisions without communicating with the central control unit or other MGs [13]. This approach helps to cope with external disturbances and can improve the robustness of the scheduling scheme, but it also makes the overall coordinated operation of the MG cluster difficult [14]. In contrast, the distributed control structure performs better in adapting to system-scale changes and communication topology adjustments, and it can better safeguard the privacy and security of each participating entity [15].

With the increasing complexity of energy systems and the intensification of data, adaptive intelligent control methods represented by MPC are gradually attracting more attention, as they can optimize system performance in uncertain environments [16]. MPC can predict the future states of the system within a finite time horizon and iteratively solve optimization problems. Meanwhile, it combines the receding horizon strategy to generate an optimal control sequence. After executing control actions at each time step, it will re-optimize based on the updated system states and prediction results [17]. This method allows for the customization of objective functions to incorporate multiple objectives, such as minimizing energy costs, reducing carbon emissions, and improving power-grid operation efficiency, into a unified optimization framework [18]. In reference [19], MPC was used to achieve multi-time-scale scheduling of integrated energy systems, with subsystems collaborating to meet control requirements. Reference [20] adopted a mathematical programming approach to construct a multi-time-scale optimal scheduling model for a hydrogen-based integrated energy system, coordinating day-ahead and intra-day scheduling. Reference [21] proposed a parameter-adaptive stochastic MPC power regulation strategy to address the uncertainties in a wind–solar–hydrogen coupled power generation system. Reference [22] developed an economic MPC method for adjusting heat consumption based on electricity price response. Reference [23] also used MPC to optimize the operation of battery energy storage systems with a 24 h rolling cycle.

In the energy trading problem, game theory has become a commonly used analytical tool, as it can effectively handle the interest distribution problem among multiple agents [24]. Reference [25] established an optimal scheduling model for a multi-MGS shared energy storage system. It uses energy storage to smooth the fluctuations of renewable energy in each MG and rationally allocates the shared capacity to improve the overall benefits of both the MG and the energy storage system. Reference [26] constructed an economic cooperative game framework that takes into account both the MG and energy storage to achieve a win–win situation for all participants. The Shapley value method is a classic cooperative game distribution method in terms of interest distribution. Reference [27] used the multi-leader–multi-follower Stackelberg game to characterize the

multilateral contract trading behavior between integrated energy service providers and load aggregators. Reference [28] also constructed an optimal scheduling model for an electricity–heat–hydrogen integrated energy system based on the Stackelberg game. Some studies have integrated scheduling-influencing factors into a correction coefficient that is incorporated it into the gain distribution model for improvement to more accurately reflect the contribution of each agent [29]. Even though this method has been improved to make the contribution of each agent more accurate, it is still difficult to avoid the combinatorial explosion problem of the Shapley value in large-scale systems [30].

Based on the advantages of the MPC and cooperative game methods, they are used to solve the above-mentioned problems.

1. In response to the uncertainties in MG energy management and the requirements for forward-looking and rational energy trading and scheduling, an optimized scheduling framework based on MPC is proposed. Through the rolling-horizon optimization and closed-loop feedback mechanism, the economy and robustness of system operation are ensured.
2. Based on cooperative game theory, a distributed trading model for interconnected MGs is constructed. The Nash model is equivalently decomposed into a two-stage problem of energy trading volume and trading price to remove the variable coupling limitation, ensuring the rationality and feasibility of trading.
3. In response to the limitations inherent in traditional distributed optimization methods, an enhanced alternating-direction method of multipliers (ADMM) is proposed. By incorporating a dynamic penalty mechanism and a parallel computing strategy, the proposed approach significantly accelerates convergence speed, making it well-suited for the coordinated optimal scheduling of large-scale MG clusters. This method effectively supports the sustainable operation of larger-scale clean energy clusters.

## 2. Overview of Interconnected Microgrid Framework and Scheduling Process

### 2.1. Microgrid Framework and Models

As shown in Figure 1, the region consists of three MGs. Each MG includes wind turbines (WTs), photovoltaic (PV) systems, gas turbines (GTs), and energy storage systems (ESSs) with different installed capacities, as well as electrical loads with varying demand levels. These MGs are directly connected to a common bus.

Within this framework, each subsystem is equipped with an independent local MPC controller. Each local MPC controller serves as a decision-making unit comprising three core components: a prediction module, an optimization objective, and a solution mechanism. The prediction module forecasts the dynamic response of the system based on given control commands. When communication between controllers is normal and mutual trust is established, they can share decision variables and control actions with each other. The optimization objective serves as the evaluation criterion for system performance. This function directly characterizes the control requirements, and since the decision variables of each controller are coupled with one another, minimizing the objective function yields the optimal strategy to meet the control goals. The solution mechanism essentially involves solving a dynamic optimization problem. Each controller determines the optimal control sequence through computation, thereby ensuring the optimal evolution of the system performance indicators.

During the iterative solution process, the distributed MPC controllers exchange real-time calculation results of the current control variables, while the global controller coordinates the optimization steps of each local controller to ensure convergence of the

iterative process. After receiving global coordination signals during each iteration, each local controller updates and shares its optimized calculation results.

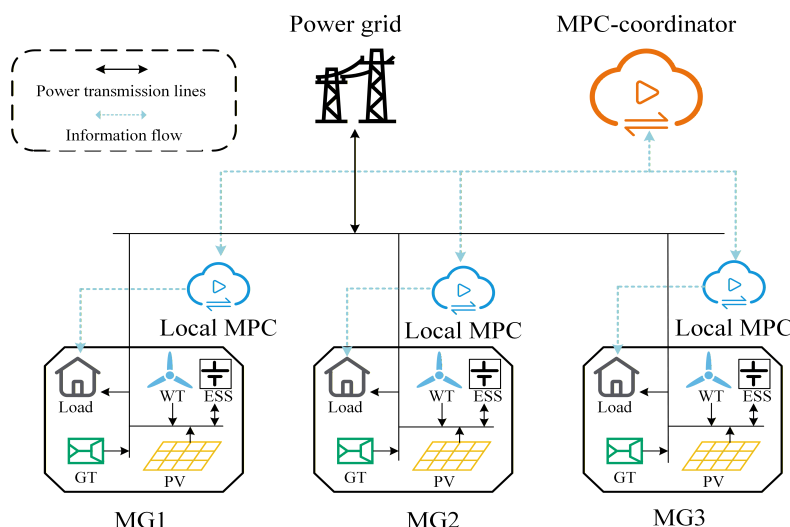


Figure 1. The overall framework of interconnected microgrids.

(1) WT and PV units:

The actual output power of the WT and PV shall not exceed the forecasted power for any given time period [7].

$$0 \leq P_{PV,i}^t \leq P_{PV,i,max}^t \tag{1}$$

$$0 \leq P_{WT,i}^t \leq P_{WT,i,max}^t \tag{2}$$

where  $P_{PV,i}^t$  and  $P_{WT,i}^t$  denote the actual output power of the photovoltaic unit and the wind turbine, respectively, and  $P_{PV,i,max}^t$  and  $P_{WT,i,max}^t$  denote the forecast maximum power of the photovoltaic unit and the wind turbine, respectively.

(2) GT units:

The GT, defined as a device for converting natural gas into electricity and heat, is modeled as follows [7]:

$$P_{GT,i}^t = \eta_{GT} G_{gas,i}^t \tag{3}$$

$$0 \leq P_{GT,i}^t \leq P_{GT,i,max} \tag{4}$$

$$D_{GT,i,min} \leq P_{GT,i}^t - P_{GT,i}^{t-1} \leq D_{GT,i,max} \tag{5}$$

where  $P_{GT,i}^t$  denotes the electrical output of GT at time  $t$ ,  $\eta_{GT}$  is its efficiency,  $G_{gas,i}^t$  is its natural gas consumption,  $P_{GT,i,max}$  is its maximum output, and  $D_{GT,i,max}$  and  $D_{GT,i,min}$  are its upward/downward ramping limits.

(3) ESS units:

The operation of the ESS can be modeled as follows [31]:

$$S_i^t = S_i^{t-1} + \eta_{cha} \cdot P_{cha,i}^t \cdot \Delta t - P_{dis,i}^t \cdot \Delta t / \eta_{dis} \tag{6}$$

$$S_{i,min}^t \leq S_i^t \leq S_{i,max}^t \tag{7}$$

where  $S_i^t$  and  $S_i^{t-1}$  denote the energy levels of the battery at time intervals  $t$  and  $t - 1$ , respectively;  $\eta_{cha}$  and  $\eta_{dis}$  represent the charging and discharging efficiencies of the battery, respectively;  $P_{cha,i}^t$  and  $P_{dis,i}^t$  are the charging and discharging powers of the battery, respectively; and  $S_{i,min}^t$  and  $S_{i,max}^t$  indicate the lower and upper limits of the battery capacity, respectively.

Within a given time period, the charging and discharging powers are constrained within certain limits:

$$0 \leq P_{cha,i}^t \leq P_{cha,i,max}^t \quad (8)$$

$$0 \leq P_{dis,i}^t \leq P_{dis,i,max}^t \quad (9)$$

where  $P_{cha,i,max}^t$  and  $P_{dis,i,max}^t$  represent the maximum allowable charging power and discharging power of the battery, respectively.

## 2.2. Interconnected Microgrid Scheduling Process Based on Cooperative Game Theory and MPC

The overall process of interconnected MG scheduling based on cooperative game theory and MPC is shown in Figure 2. First, the control horizon, prediction horizon, and time are initialized. Then, the predicted electricity and heat demands, as well as the forecasted wind and photovoltaic power generation, are taken as inputs. A multi-MG transaction model is established based on cooperative game theory, and a two-stage decoupled optimization model, along with the ADMM distributed algorithm, is used to solve the first-stage subproblems, obtaining the transaction power between each MG and other MGs, as well as the distribution network. The MPC strategy is introduced to make decisions on unit output and optimize power transactions. This process continues until  $t = 24$ , when transaction volumes are finalized. Then, the second-stage subproblems are solved using the ADMM algorithm to determine transaction prices among MGs. Finally, the scheduling decisions for each MG, inter-MG transaction power, and transaction prices are output, achieving distributed cooperative optimization and marketized trading among multiple MGs.

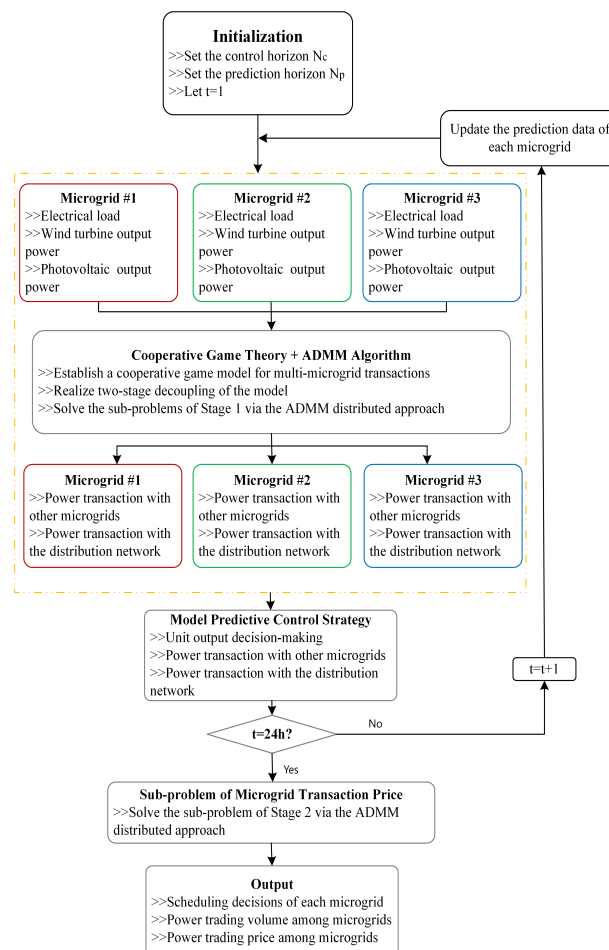


**Figure 2.** The overall process of interconnected microgrid scheduling based on cooperative game theory and model predictive control.

### 3. Microgrid Optimization Model

#### 3.1. Objective Function

To enhance the utilization of renewable energy and improve the overall economic efficiency of an MG integrating renewable energy generation, battery storage, and load, the following objective function is established under the constraints of meeting energy balance relationships and operational requirements.

$$C_i = C_{g,i} + C_{e,i} + C_{yw,i} + C_{trade,i}, \quad (10)$$

where  $C_{g,i}$  represents the gas purchase cost,  $C_{e,i}$  represents the cost of electricity purchase and sale,  $C_{yw,i}$  represents the operation and maintenance cost of the units, and  $C_{trade,i}$  represents the transaction cost between the  $i$ -th MG and other MGs.

The mathematical model for the gas purchase cost is expressed as follows:

$$C_{g,i} = \sum_{t=\tau}^{\tau+N_p} (k_{g,t} G_{gas,i}^t), \quad (11)$$

where  $k_{g,t}$  is the gas purchase price at time  $t$ ,  $G_{gas,i}^t$  is the gas purchase amount at time  $t$ ,  $\tau$  is the current time period, and  $N_p$  is the prediction horizon.

The mathematical model for electricity purchase and sale costs is expressed as follows:

$$C_{e,i} = \sum_{t=\tau}^{\tau+N_p} (k_{buy}^t P_{buy,i}^t - k_{sell}^t P_{sell,i}^t), \quad (12)$$

where  $P_{buy,i}^t$  is the electricity purchase amount at time  $t$ ,  $P_{sell,i}^t$  is the electricity sale amount at time  $t$ , and  $k_{buy}^t$  and  $k_{sell}^t$  are the electricity purchase and sale prices at time  $t$ , respectively.

The operation and maintenance cost of the units is expressed as follows:

$$C_{yw,i} = \sum_{t=\tau}^{\tau+N_p} (k_{GT} P_{GT,i}^t + k_{WT} P_{WT,i}^t + k_{PV} P_{PV,i}^t), \quad (13)$$

where  $P_{GT,i}^t$  represents the output power of the GT unit at time interval  $t$ ,  $P_{WT,i}^t$  represents the output power of the WT at time interval  $t$ ,  $P_{PV,i}^t$  represents the output power of the PV at time interval  $t$ ,  $k_{GT}$  is the operation and maintenance coefficient of the GT unit,  $k_{WT}$  is the operation and maintenance coefficient of the wind turbine, and  $k_{PV}$  is the operation and maintenance coefficient of the photovoltaic system.

The mathematical model for electricity trading is expressed as follows:

$$C_{trade,i} = - \sum_{t=\tau}^{\tau+N_p} \sum_{j=1/i}^N k_{trade,ij}^t P_{trade,ij}^t, \quad (14)$$

where  $P_{trade,ij}^t$  is the electricity trade volume between the  $i$ -th MG and other MGs at time  $t$ ,  $k_{trade,ij}^t$  is the electricity trade price between the  $i$ -th MG and other MGs at time  $t$ , and  $N$  is the number of MGs.

#### 3.2. Constraints

In addition to the constraints of the unit models described in Equations (1)–(9), the operation of interconnected MGs must also satisfy the following constraints:

(1) Power balance constraint:

$$P_{GT,i}^t + P_{dis,i}^t + P_{WT,i}^t + P_{PV,i}^t + P_{buy,i}^t = P_{sell,i}^t + P_{cha,i}^t + \sum_{j=1/i}^N P_{trade,ij}^t + P_{L,i}^t \quad (15)$$

where  $P_{L,i}^t$  represents the electrical load at time interval  $t$ .

(2) Electricity purchase and sale constraint:

Due to the limited capacity of transmission lines, the electricity transaction volume between the MG and the grid must satisfy the following constraints:

$$\begin{cases} P_{m,i,\min}^t \leq P_{buy,i}^t \leq P_{m,i,\max}^t \\ P_{m,i,\min}^t \leq P_{sell,i}^t \leq P_{m,i,\max}^t \end{cases}, \quad (16)$$

where  $P_{m,i,\max}^t$  and  $P_{m,i,\min}^t$  represent the upper and lower limits of electricity transactions between the MG and the grid, respectively.

(3) Electricity transaction volume constraint:

$$P_{trade,\min}^t \leq P_{trade,ij}^t \leq P_{trade,\max}^t \quad (17)$$

$$\sum_{i=1}^N \sum_{j=1/i}^N P_{trade,ij}^t = 0, \quad (18)$$

where  $P_{trade,\max}^t$  and  $P_{trade,\min}^t$  represent the upper and lower limits of electricity transactions between MGs, respectively.

(4) Electricity trading price constraint:

The electricity trading price between MGs should fall between the electricity purchase and sale prices of the distribution network.

$$k_{sell}^t \leq k_{trade,ij}^t \leq k_{buy}^t \quad (19)$$

#### 4. MPC Strategy

During the optimization process, sudden disturbances, such as random fluctuations on both the source and load sides that may occur in the system, can affect the real-time processing performance of MPC. To address this situation, parameters such as the MPC sampling period and control horizon are dynamically adjusted to improve the optimization accuracy.

Due to the uncertainties in load demand and the power prediction of wind and photovoltaic generation, the actual output deviation exhibits random fluctuation characteristics. To address the issue of determining the fluctuation range of such prediction deviations, the quantile regression method is employed for recursive calculation. Finally, the load interval  $[-\Delta P_{L,i}^t, \overline{\Delta P_{L,i}^t}]$ , the photovoltaic output fluctuation interval  $[-\Delta P_{PV,i}^t, \overline{\Delta P_{PV,i}^t}]$ , and the wind power output fluctuation interval  $[-\Delta P_{WT,i}^t, \overline{\Delta P_{WT,i}^t}]$  of each MG during period  $t$  are obtained.

In view of the insufficient adaptability of the optimization process caused by the fixed step sizes of the prediction and control horizons in MPC, this paper adopts an improved algorithm strategy with dynamic adjustment. Considering the time-varying characteristics of the prediction errors of wind power, photovoltaic power output, and load demand, this method can dynamically and adaptively adjust the step sizes of the prediction and control horizons, track the prediction deviations of variables in real time, and automatically adjust the parameters in each rolling optimization cycle. To balance the computational efficiency and optimization performance, the step sizes of the two horizons need to be kept consistent. For a system with an initial step size, the step sizes are as follows:

$$q = \frac{\Delta P_{L,i}^t}{P_{L,i}^t} + \frac{\Delta P_{PV,i}^t}{P_{PV,i}^t} + \frac{\Delta P_{WT,i}^t}{P_{WT,i}^t}, \tag{20}$$

$$N_t = N_0 - Z(q), \tag{21}$$

$$Z(q) = \begin{cases} 0, & 0 < q \leq q_1, \\ 1, & q_1 < q \leq q_2, \\ N_0 - 1, & q > q_n, \end{cases} \tag{22}$$

where  $\Delta P_{L,i}^t = \max\{-\Delta P_{L,i}^t, \overline{\Delta P_{L,i}^t}\}$ ;  $\Delta P_{PV,i}^t = \max\{-\Delta P_{PV,i}^t, \overline{\Delta P_{PV,i}^t}\}$ ,  $\Delta P_{WT,i}^t = \max\{-\Delta P_{WT,i}^t, \overline{\Delta P_{WT,i}^t}\}$ ,  $P_{L,i}^t$ ,  $P_{PV,i}^t$  and  $P_{WT,i}^t$  are the day-ahead predicted values of the load, wind power and photovoltaic power of each microgrid in period  $t$ , respectively; and  $q_1, q_2, \dots, q_n$  are the interval demarcation values of  $q$ .

The time-interval adjustment mechanism of adaptive sampling is based on the following design criteria.

$$\begin{cases} u_t = u_0 - e_s, \\ v_s = \left| \frac{\sum_{k=1}^{u_0 - e_s} P_{uc,k,i}}{r_0 - e_s} \right| - P_{uc,1,i} & v_{s,\min} \leq v_s \leq v_{s,\max}, \\ e_s = v_s^{-1} & 0 \leq e_s \leq u_t - 1, \end{cases} \tag{23}$$

$$\Delta T = u_t \Delta T_s, \tag{24}$$

$$P_{uc,i}^0 = P_{L,i}^0 + P_{PV,i}^0 + P_{WT,i}^0, \tag{25}$$

$$P_{uc,i}^k = P_{L,i}^k + P_{PV,i}^k + P_{WT,i}^k, \tag{26}$$

where  $u_t$  is the sampling step size in time period  $t$ ;  $u_0$  is the initial sampling step size;  $v_{s,\min}$  and  $v_{s,\max}$  are the upper and lower limits of the fluctuation;  $P_{L,i}^0$ ,  $P_{WT,i}^0$  and  $P_{PV,i}^0$  are the actual values of the  $i$ -th MG's load, photovoltaic power generation, and wind power grid in time period  $t$ , respectively; and  $P_{L,i}^k$ ,  $P_{PV,i}^k$  and  $P_{WT,i}^k$  are the values of the load, photovoltaic power generation, and wind power generation at the  $k$ -th sampling point of the  $i$ -th MG in time period  $t$ , respectively.

The dynamic characteristics of the  $i$ -th MG in the alliance can be described by the following discrete-time state-space equations:

$$\chi_i^{t+1} = A_i \chi_i^t + B_i u_i^t + D_i w_i^t + \sum_{i \neq j} A_{ij} \chi_j^t, \tag{27}$$

$$\gamma_i^t = C_i Y_i^t, \tag{28}$$

where  $A_i$  is the state matrix;  $\chi_i^t$  is the state variable, including the state of charge of the ESS ( $S_i^t$ );  $B_i$  is the control matrix;  $u_i^t$  is the control variable, including the power of electricity trading between MGs ( $P_{trade,ij}^t$ ), the power of trading between the MG and the upper-level power grid ( $P_{buy,i}^t, P_{sell,i}^t$ ), the charging and discharging power of the ESS ( $P_{cha,i}^t, P_{dis,i}^t$ ) and the GT power ( $P_{GT,i}^t$ );  $D_i$  is the disturbance matrix;  $w_i^t$  is the disturbance variable, including the load ( $\Delta P_{L,i}^t$ ), the wind power ( $\Delta P_{WT,i}^t$ ) and the photovoltaic power ( $\Delta P_{PV,i}^t$ );  $A_{ij}$  is the information matrix between the  $i$ -th MG and the  $j$ -th MG;  $C_i$  is the output matrix ( $Y_i^t$ ), including  $P_{GT,i}^t, P_{dis,i}^t, P_{WT,i}^t, P_{PV,i}^t, P_{buy,i}^t, P_{sell,i}^t, P_{cha,i}^t, P_{trade,ij}^t$  and  $S_i^t$ .

### 5. Interconnected Microgrid Cooperative Game Operation Optimization Cooperative Game Modeling

The construction of the asymmetric Nash bargaining model is expressed as follows:

$$\begin{cases} \max \prod_{i=1}^N (C_i^0 - C_i)^{w_i}, \\ \text{s.t. } C_i \leq C_i^0, \end{cases} \quad (29)$$

where  $N$  represents the number of MGs in the alliance,  $C_i^0$  is the operating cost of an MG when it operates independently, and  $C_i$  is the operating cost of the  $i$ -th MG after the cooperative game among multiple MGs. The constraint condition ( $C_i \leq C_i^0$ ) indicates that the operating cost after cooperation is less than that before cooperation, and  $w_i$  represents the contribution rate of MG  $i$  within the alliance.

The above problem is transformed into two convex subproblems: the minimum operational cost subproblem and the transaction bargaining subproblem.

Subproblem 1: Minimum operational cost subproblem.

$$\min \sum_{i=1}^N (C_{g,i} + C_{e,i} + C_{yw,i}), \quad (30)$$

By solving the above equations, the optimal electricity transaction volume among different MGs can be obtained.

Subproblem 2: Transaction bargaining subproblem.

$$\max \sum_{i=1}^N w_i \ln(C_i^0 - C_i), \quad (31)$$

In this paper, a nonlinear function based on the natural logarithm is employed to quantify the contribution of the MG. The process of contribution quantification is described as follows:

First, calculate the total supply and acquired energy of each MG in the cooperative game, as well as the upper limits of supply and acquisition for each MG.

$$\begin{cases} E_i^s = \sum_{t=1}^T \sum_{i=1}^N \left\{ \max(0, P_{trade,ij}^t) \right\}, i \neq j, \\ E_i^r = \sum_{t=1}^T \sum_{i=1}^N \left\{ \min(0, P_{trade,ij}^t) \right\}, i \neq j, \\ E_{\max}^s = \max(E_i^s), \\ E_{\max}^r = \max(E_i^r), \end{cases} \quad (32)$$

where  $E_i^s$  represents the energy provided by each MG through the coalition cooperative game,  $E_i^r$  represents the energy obtained by the MG through the coalition cooperative game, and  $E_{\max}^s$  and  $E_{\max}^r$  are the maximum values that each MG can provide and obtain during the cooperative game process.

The contribution degree ( $W_i$ ) of each MG is quantified by an exponential function based on the natural constant ( $e$ ) as follows:

$$w_i = e^{E_i^s / E_{\max}^s} - e^{-(E_i^r / E_{\max}^r)}, \quad (33)$$

## 6. Solution Steps of the Bargaining Model Based on ADMM

The ADMM algorithm is employed to solve the minimum operational cost subproblem and the transaction bargaining subproblem.

(1) Solution flow for Subproblem 1:

First, it is necessary to determine the optimal electricity trading volume among the MGs, then decouple the electricity transactions between the MGs:

$$P_{trade,ij}^t = P_{trade,ji}^t \tag{34}$$

where  $P_{trade,ij}^t$  represents the expected electricity transaction volume between the  $i$ -th MG and the  $j$ -th MG and  $P_{trade,ji}^t$  represents the expected electricity transaction volume between the  $j$ -th MG and the  $i$ -th MG.

Substitute the optimization objective function of the MG into the augmented Lagrange function formula to obtain the augmented Lagrange function of the  $i$ -th MG in Subproblem 1:

$$\min L_i^1 = C_{g,i} + C_{e,i} + C_{yw,i} + \sum_{j=1/i}^N \left( \lambda_{ij}^t (P_{trade,ij}^t - P_{trade,ji}^t) + \frac{\rho_1}{2} \|P_{trade,ij}^t - P_{trade,ji}^t\|_2^2 \right), \tag{35}$$

where  $\lambda_{ij}^t$  and  $\rho_1$  are the Lagrange multiplier and the penalty factor for the minimum coalition operation cost problem, respectively.

Augmented Lagrange function of the  $j$ -th MG:

$$\min L_j^1 = C_{g,j} + C_{e,j} + C_{yw,j} + \sum_{i=1/j}^N \left( \lambda_{ij}^t (P_{trade,ji}^t - P_{trade,ij}^t) + \frac{\rho_1}{2} \|P_{trade,ji}^t - P_{trade,ij}^t\|_2^2 \right). \tag{36}$$

The Lagrange multiplier mentioned above is updated as follows:

$$\lambda_{ij}^{t,k+1} = \lambda_{ij}^{t,k} + \rho_1 (P_{trade,ij}^{t,k+1} - P_{trade,ji}^{t,k+1}) \tag{37}$$

The solution steps of the subproblem for minimizing the operation cost of the MG coalition are outlined as follows:

- (1) Initialize the iteration number as  $k = 0$  and the penalty factor as  $\rho_1 = 10^{-3}$ . The convergence precision of both the primal residual and dual residual is set to  $10^{-4}$ , and the initial Lagrange multiplier is  $\lambda_{ij}^t = 0$ . The power transaction volume in the first iteration is  $P_{trade,ij}^{t,k} = P_{trade,ji}^{t,k} = 0$ .
- (2) the  $i$ -th MG obtains electric energy from the  $j$ -th MG ( $P_{trade,ji}^{t,k}$ ); then, the expected power transaction volume is obtained by solving Equation (35) ( $P_{trade,ij}^{t,k+1}$ ).
- (3) The  $j$ -th MG obtains electric energy from the  $i$ -th MG ( $P_{trade,ij}^{t,k+1}$ ); then, the expected power transaction volume is obtained by solving Equation (36) ( $P_{trade,ji}^{t,k+1}$ ).
- (4) The Lagrange multiplier is updated using Equation (37), and the iteration count is updated as  $k = k + 1$ .
- (5) The convergence of the algorithm is judged using the primal residual and dual residual:

$$\begin{cases} \sum_{t=1}^T \sum_{i=1}^N \sum_{j=1/i}^N \|P_{trade,ij}^{t,k} - P_{trade,ji}^{t,k}\|_2 \leq \epsilon_1^{pri} \\ \sum_{t=1}^T \sum_{i=1}^N \sum_{j=1/i}^N \|P_{trade,ij}^{t,k+1} - P_{trade,ji}^{t,k+1}\|_2 \leq \epsilon_1^{dual} \end{cases} \tag{38}$$

- (6) If the convergence condition is satisfied in Step 5, the iteration stops. Otherwise, return to Step 2 and iterate again until the convergence condition is met or the maximum number of iterations is reached.

(2) Solution flow of Subproblem 2:

After determining the optimal power transaction volume of each MG, decouple the electricity transaction prices between each MG:

$$k_{trade,ij}^t = k_{trade,ji}^t \quad (39)$$

where  $k_{trade,ij}^t$  is the expected transaction price between the  $i$ -th MG and the  $j$ -th MG and  $k_{trade,ji}^t$  is the expected transaction price between the  $j$ -th MG and the  $i$ -th MG.

The corresponding augmented Lagrangian function for the  $i$ -th MG and the  $j$ -th MG is expressed as follows:

$$\begin{cases} \min L_i^2 = -w_i \ln(C_i^0 - C_i) + \sum_{j=1/i}^N \left( \zeta_{ij}^t (k_{trade,ij}^t - k_{trade,ji}^t) + \frac{\rho_2}{2} \|k_{trade,ij}^t - k_{trade,ji}^t\|_2^2 \right) \\ s.t. C_i^0 - C_i \geq 0 \end{cases} \quad (40)$$

$$\begin{cases} \min L_j^2 = -w_j \ln(C_j^0 - C_j) + \sum_{i=1/j}^N \left( \zeta_{ij}^t (k_{trade,ji}^t - k_{trade,ij}^t) + \frac{\rho_2}{2} \|k_{trade,ji}^t - k_{trade,ij}^t\|_2^2 \right) \\ s.t. C_j^0 - C_j \geq 0 \end{cases} \quad (41)$$

where  $\zeta_{ij}^t$  and  $\rho_2$  are the Lagrange multiplier and penalty factor, respectively. The Lagrange multiplier is updated as follows:

$$\zeta_{ij}^{t,k+1} = \zeta_{ij}^{t,k} + \rho_2 (k_{trade,ij}^{t,k} - k_{trade,ji}^{t,k}) \quad (42)$$

The specific steps of Subproblem 2 are outlined as follows:

- (1) Set the initial number of iterations as  $k = 0$  and the penalty factor as  $\rho_2 = 10^{-3}$ . The convergence accuracy of both the primal residual and dual residual is  $10^{-4}$ , the initial Lagrange multipliers are  $\zeta_{ij}^{t,k} = 0$ , and the expected payment for the first iteration is  $k_{trade,ij}^t = k_{trade,ji}^t = 0$ .
- (2) For the  $i$ -th MG, obtain the transaction price from the  $j$ -th MG ( $k_{trade,ji}^{t,k}$ ), then solve Equation (40) to obtain the expected transaction price of the  $i$ -th MG ( $k_{trade,ij}^{t,k+1}$ ).
- (3) For MG  $j$ , obtain the transaction price from MG  $i$  ( $k_{trade,ij}^{t,k+1}$ ), then solve Equation (41) to obtain the expected transaction price of MG  $j$  ( $k_{trade,ji}^{t,k+1}$ ).
- (4) Update the Lagrange multiplier using Equation (42) and update the iteration number as  $k = k + 1$ .
- (5) Judge the convergence of the algorithm using the primal residual and dual residual:

$$\begin{cases} \sum_{t=1}^T \sum_{i=1}^N \sum_{j=1/i}^N \|k_{trade,ij}^{t,k+1} - k_{trade,ji}^{t,k+1}\|_2 \leq \varepsilon_2^{pri} \\ \sum_{t=1}^T \sum_{i=1}^N \sum_{j=1/i}^N \|k_{trade,ij}^{t,k+1} - k_{trade,ij}^{t,k}\|_2 \leq \varepsilon_2^{dual} \end{cases} \quad (43)$$

- (6) If the convergence condition is satisfied in Step 5, stop the iteration. Otherwise, return to Step 2 and iterate again until the convergence condition is met or the maximum number of iterations is reached.

## 7. Results and Discussion

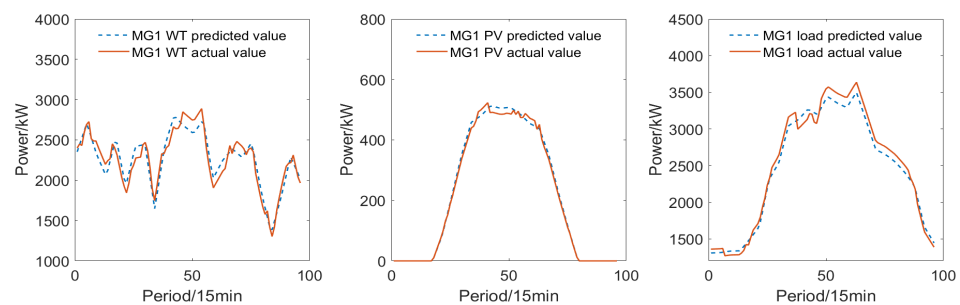
To analyze the effectiveness of the multi-stage, multi-time-scale and cooperative game optimization control method proposed in this paper, two scenarios are set up for simulation and analysis. The scenarios involve three MGs. The load and renewable energy output

within the MGs are shown in Figures 3–5. The renewable energy sources in MG1 include photovoltaics and wind power, while those in MG2 and MG3 are photovoltaic. The electricity purchase price from the power grid is shown in Figure 6. The overall fluctuation range of the real price is relatively large, and the overall trend of the predicted value is highly consistent with the real value, effectively capturing the periodic fluctuation characteristics of the price. The price of natural gas is 3.5 CNY/m<sup>3</sup>. The operation and maintenance costs for wind turbines, photovoltaic panels, and gas turbines are 0.2 CNY/kWh, 0.15 CNY/kWh, and 0.3 CNY/kWh, respectively. The electricity selling price of the upstream grid is shown in Figure 6, and the feed-in tariff is set to half of the selling price. The equipment parameters of the MGs are shown in Table 1. The control horizon of the MPC algorithm corresponds to a scheduling time resolution of 15 min. Accordingly, a 24 h operation cycle is divided into 96 scheduling intervals, with a prediction horizon of 16 steps. The initial state of charge of the energy storage system is set at 50% of its rated capacity. The code was developed in MATLAB 2019a, modeled with YALMIP, and solved by CPLEX. The computing environment is a PC with an Intel Core i7-1355U 5.0 GHz CPU and 8 GB of RAM.

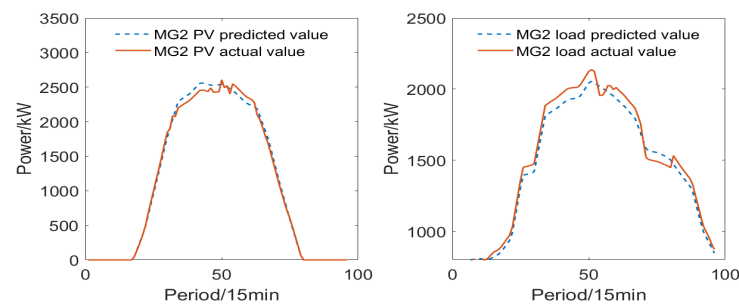
Scenario 1: Each MG operates in cooperation, adopting the methods of MPC and cooperative game theory.

Scenario 2: Each MG operates independently.

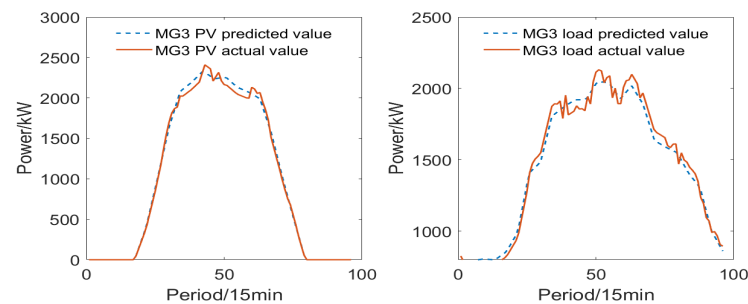
Scenario 3: Each MG operates in a cooperative manner without considering MPC.



**Figure 3.** Forecasted and actual power of sources and loads in microgrid 1.



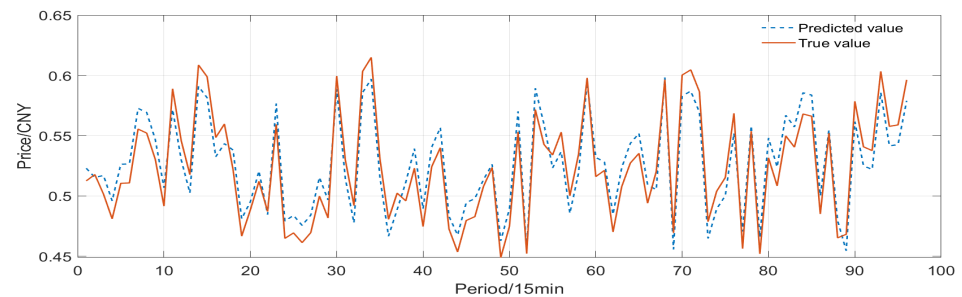
**Figure 4.** Forecasted and actual power of sources and loads in microgrid 2.



**Figure 5.** Forecasted and actual power of sources and loads in microgrid 3.

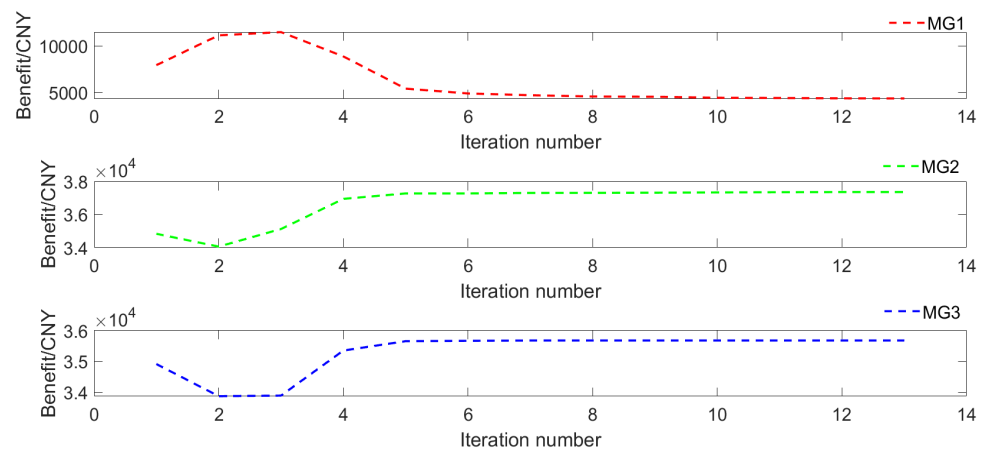
**Table 1.** Equipment parameters of microgrids.

Parameter	MG1	MG2	MG3
Maximum output power of GT	500 kW	500 kW	500 kW
Minimum output power of GT	0 kW	0 kW	0 kW
Power generation efficiency of GT	0.35	0.35	0.35
Maximum charging power of ESS	500 kW	500 kW	500 kW
Maximum discharging power of ESS	500 kW	500 kW	500 kW
Charging efficiency of ESS	0.95	0.95	0.95
Discharging efficiency of ESS	0.95	0.95	0.95
Maximum capacity of ESS	500 kW	500 kW	500 kW
Minimum capacity of ESS	100 kW	100 kW	100 kW
Maximum power interaction with the grid	8000 kW	8000 kW	8000 kW



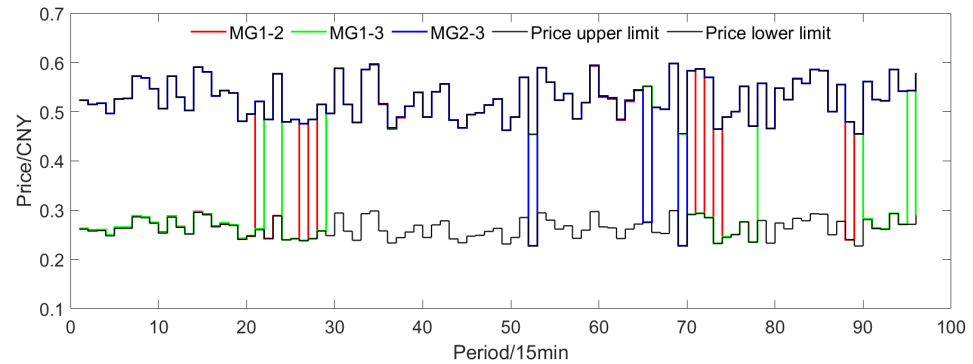
**Figure 6.** Grid electricity price.

Figure 7 shows the iterative convergence during the optimization process based on MPC. The benefit functions of the three MGs all converge within a finite number of iterative steps. The benefit of MG1 rises rapidly in the first few iterations, then tends to be stable, while MG2 and MG3 enter the stable stage after the fourth and sixth iterations, respectively.



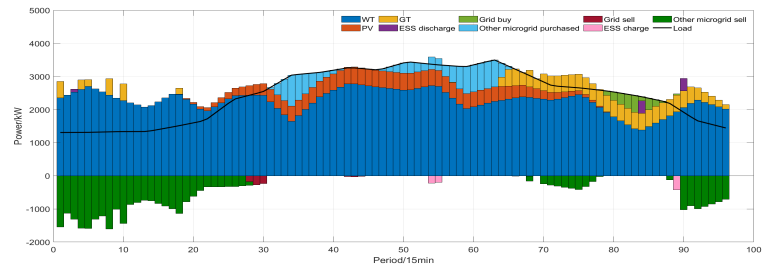
**Figure 7.** Iterative convergence curve.

As shown in Figure 8, the trading price between MGs fluctuates within the range of 0.35–0.55 yuan/kWh, always remaining lower than the electricity purchase price from the power grid and higher than the electricity selling price to the power grid. Cooperative trading between MGs can effectively reduce the electricity purchase cost. The energy complementarity between MGs weakens the impact of power-grid electricity price fluctuations on the operational economy of a single MG and enhances the overall robustness and economy of the system.

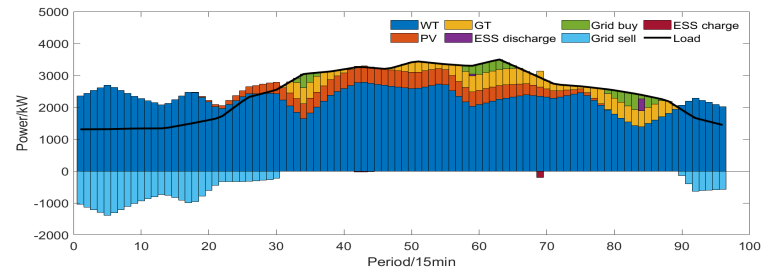


**Figure 8.** Electricity trading price between microgrids.

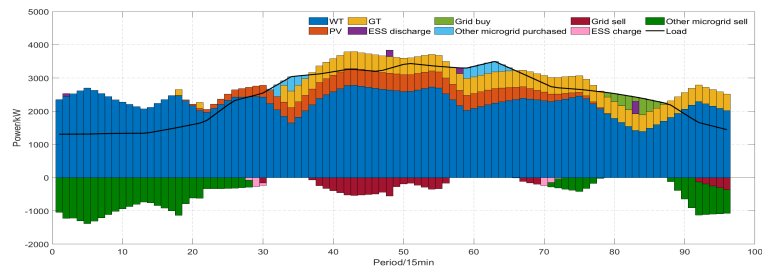
Figures 9–11 show the active power-balance results of MGs in Scenarios 1, 2, and 3. Scenario 1 adopts the coordinated scheduling strategy combining MPC and cooperative game theory; Scenario 2 corresponds to the independent operation of each MG; and Scenario 3 only considers cooperative game theory. This scenario setting is consistent with most existing studies. By comparing scenarios with and without MPC, it can be seen that MG1 with MPC hardly require gas-turbine generation during scheduling periods 32–69, instead purchasing more electricity from other MGs. This is because, without MPC, the optimization only targets the minimization of the current operating cost, without considering the predicted information of future periods and the global cooperative benefits, therefore relying more on GT generation to meet the immediate load requirement. During periods 38–57, the operation scenario without MPC increases GT output and sells more electricity to the main grid for relatively low profits. This is because the scheduling strategy without MPC only takes the economic benefit of a single period as the optimization objective. To maximize the profit of that period, it increases the gas turbine output to generate surplus electricity, which is then sold to the main grid for revenue. This mode only pursues the local optimum of the current period and does not predict the operating status and interaction costs in future periods, which easily leads to excessive local unit generation and heavy dependence on the main grid for power exchange. After introducing MPC, rolling optimization and global decision-making can be carried out based on the load, renewable energy output, electricity price, and interaction potential among multiple MGs over multiple future periods. Comparing the scenario with MPC and cooperative game theory with the independent MG operation scenario, it can be observed that during periods 0–28 and 90–96, the coordinated operation scenario sells surplus power to other MGs for revenue, whereas the independently operating MG can only sell electricity to the main grid for lower profits. During periods 31–40 and 57–65, the electric load demand is high, and the combined output of renewable energy and GT can hardly meet the load. Therefore, it is necessary to purchase electricity from external sources. The scenario with MPC and cooperative game theory satisfies the load by purchasing electricity from other MGs, while the independently operating MG can only buy power from the main grid. The cooperative operation mode reduces the dependence on the main grid and optimizes the ESS operation strategy, resulting in more balanced charging and discharging of the ESS and a more prominent peak-shaving and valley-filling effect. By leveraging the energy complementarity among multiple MGs, the cooperative operation mode improves the accommodation level of renewable energy, reduces the system's dependence on the main grid, and lowers the overall operating cost. The operating characteristics of MG2 and MG3 under each scenario are similar to those of MG1 and will not be repeated here.



(a) Scenario 1

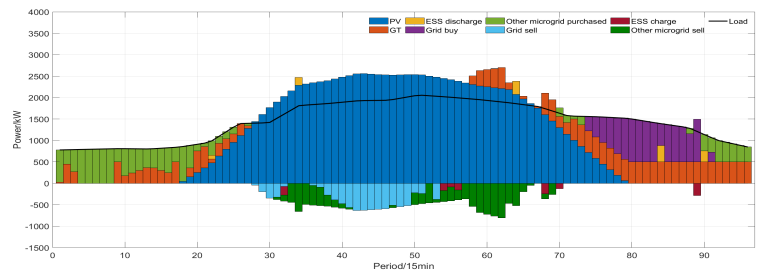


(b) Scenario 2

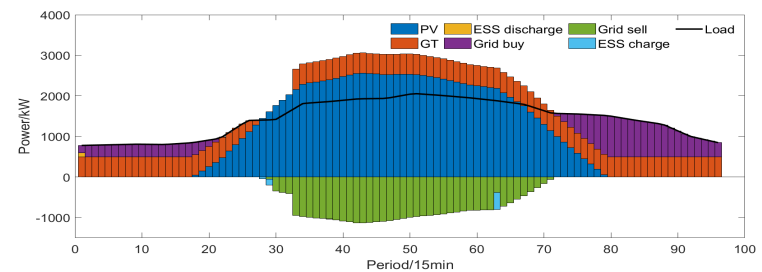


(c) Scenario 3

Figure 9. Results of power balance of MG1 in Scenarios 1, 2 and 3.

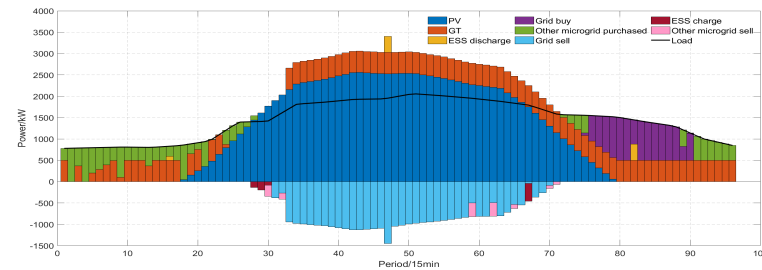


(a) Scenario 1

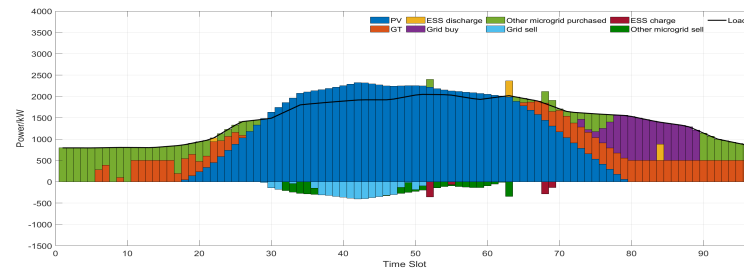


(b) Scenario 2

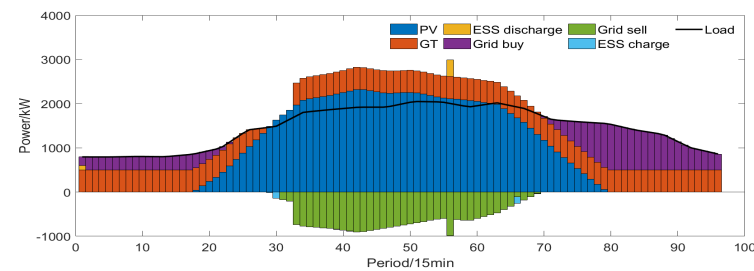
Figure 10. Cont.



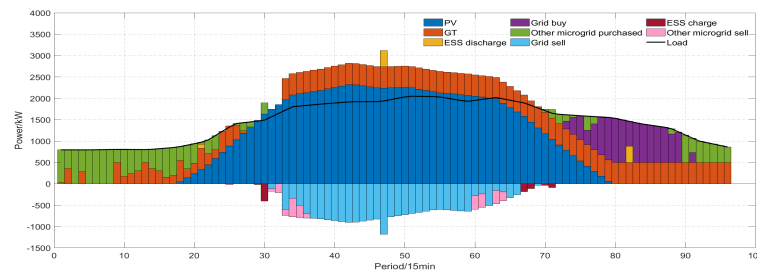
(c) Scenario 3

**Figure 10.** Results of power balance of MG2 in Scenarios 1, 2 and 3.

(a) Scenario 1



(b) Scenario 2



(c) Scenario 3

**Figure 11.** Results of power balance of MG3 in Scenarios 1, 2 and 3.

The cooperative operation mode reduces the dependence on the power grid and improves the energy storage operation strategy. The charging and discharging of the energy storage system become more balanced, and the function of peak shaving and valley filling becomes more prominent. The cooperative operation mode leverages the advantage of energy complementarity among multiple MGs to enhance the consumption level of renewable energy, reducing the system's dependence on the power grid and operating costs.

As shown in Figure 12, during the night, the wind power generation in MG1 is relatively abundant, and the load within the MG cannot fully absorb it. Therefore, the electricity is sold to other MGs to obtain higher profits, while other MGs purchase electricity from MG1 to save costs. At noon, the photovoltaic power generation in MG2 and MG3 is sufficient, and the surplus electricity is sold to MG1 for profit. The energy complementarity

among MGs is fully demonstrated. This dynamic power interaction effectively enhances the overall flexibility of the system and the utilization rate of resources, reducing the operating cost while improving the reliability of energy supply.

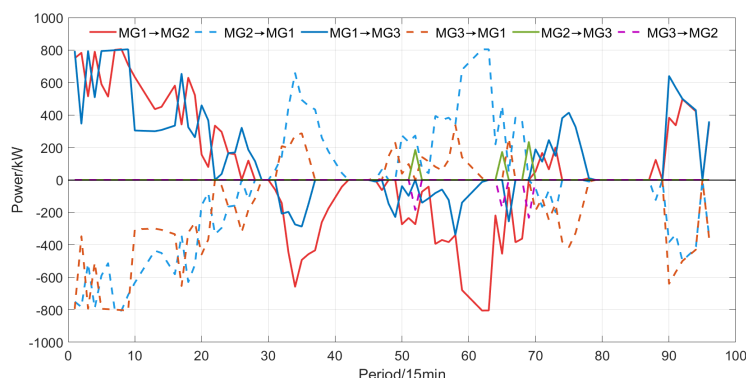


Figure 12. Bidirectional power exchange between microgrids.

It can be seen from Figure 13 that under the proposed MPC and cooperative game coordinated scheduling strategy, the comprehensive operating costs of MG1, MG2, and MG3 are all lower than those of the two most common modes in recent studies, i.e., the sole cooperative game mode and the independent operation mode. Specifically, compared with the sole cooperative game mode, the cost of MG1 is reduced by 1045 yuan, and the cost is reduced by 2965 yuan compared with independent operation, while the cost of MG2 is reduced by 1470 yuan and 7706 yuan, respectively, and the cost of MG3 is reduced by 2566 yuan and 11,650 yuan, respectively. This indicates that after introducing MPC rolling optimization on the basis of traditional cooperative game theory, the economic performance of each MG is further improved, and the proposed method is superior to existing cooperative scheduling and independent scheduling methods. From the perspective of cost composition, cooperative operation effectively reduces the interaction cost between MGs and the main grid and further optimizes the gas cost, as well as equipment operation and maintenance costs, etc. The power purchase cost of MG1 from the grid increases slightly, mainly because its surplus renewable energy is more involved in mutual power assistance among MGs and is preferentially supplied to other MGs, thereby improving the global revenue. Through energy complementarity and coordinated scheduling among multiple MGs, the proposed method realizes cross-period and cross-agent resource sharing, reduces the redundancy and power fluctuation of system operation, and achieves better overall economic performance, fully demonstrating the superiority and effectiveness of the proposed MPC and cooperative game combined scheduling strategy.

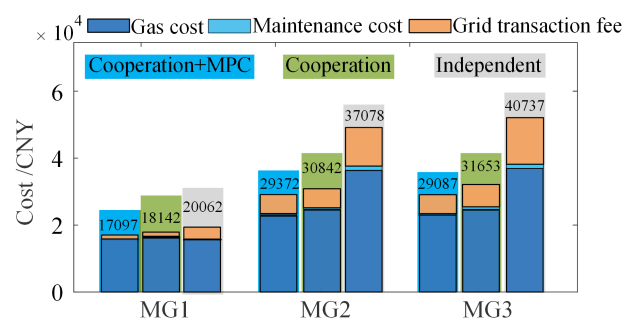
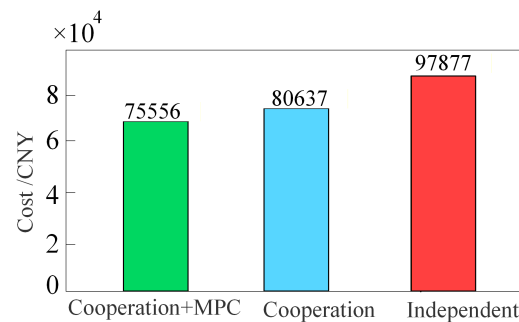


Figure 13. Comparison of costs under independent and cooperative operations.

As can be seen from Figure 14, the total cost of the system in the cooperative operation mode with MPC is 75,556 yuan, which is lower than the 80,637 yuan cost in the

cooperative operation mode without considering MPC and the 97,877 yuan cost in the independent operation mode. The interconnection and collaborative optimization among MGs not only reduce the operating pressure of individual MGs but also enable the entire system to achieve economies of scale and improve energy utilization efficiency. In addition, from a sustainability perspective, the proposed cooperative MPC-based strategy facilitates better local accommodation of renewable energy, reduces dependence on electricity purchased from the upstream grid, and supports more flexible and resilient operation of interconnected MGs.



**Figure 14.** Comparison of total operating costs.

## 8. Conclusions

This paper focuses on the problems of high operation cost, high volatility, and insufficient utilization of renewable energy caused by the independent operation of multiple MGs. A distributed cooperative energy management strategy for interconnected MGs based on MPC is proposed. This strategy combines receding-horizon optimization with a cooperative game mechanism to achieve energy complementarity and power coordination among multiple MGs, in addition to ensuring system scalability and convergence under a distributed optimization framework.

Simulation results show that under the cooperative operation mode, bidirectional power exchange can be carried out among MGs, which improves the accommodation level of renewable energy and reduces the total system operation cost by 22,321 yuan. Iterative convergence analysis verifies that the proposed ADMM algorithm guarantees solution accuracy while achieving a fast convergence rate, making it suitable for the optimal scheduling of large-scale MG clusters.

However, this method has some limitations. It was developed under the assumption that the communication between MGs is always reliable, but in practical applications, the existence of communication faults or delays will affect the system's performance. Future research can consider the robustness of the method under communication uncertainty and delays. The model proposed in this paper was simulated and verified based on a fixed MG cluster. With the development of MGs and the integration of more distributed energy sources, the scalability of the system may become a challenge. Future research can focus on exploring the scalability of the proposed method when the number of MGs or the scale of the interconnected system increases. Machine learning technologies can be integrated to adaptively adjust optimization parameters based on changing grid configurations to further improve the scalability of the system.

From the perspective of sustainability, the distributed cooperative energy management strategy for interconnected MGs based on MPC proposed in this paper not only improves the economic performance of system operation but also reduces the dependence on the upstream grid and conventional generation units by promoting bidirectional energy sharing among MGs and local consumption of renewable energy, thereby enhancing energy utilization efficiency and reducing potential environmental burdens. Meanwhile, the

adopted distributed cooperative optimization framework takes into account the flexibility, scalability, and operational resilience of multi-MG systems, enabling them to maintain more stable and efficient operation under uncertain conditions. Therefore, the contributions of this paper are reflected not only in reducing operating costs and improving scheduling performance but also in providing methodological support for the building of cleaner, more efficient, and more resilient regional energy systems with high penetration of renewable energy, demonstrating relevance to the journal's sustainability theme.

**Author Contributions:** X.Z.: investigation, conceptualization, methodology, and software; Z.L.: investigation, conceptualization, methodology, validation, and writing—review and editing; writing—original draft and writing—review and editing; C.W.: investigation, conceptualization, methodology, and validation. All authors have read and agreed to the published version of the manuscript.

**Funding:** This research received no external funding.

**Institutional Review Board Statement:** Not applicable.

**Informed Consent Statement:** Not applicable.

**Data Availability Statement:** No new data were created or analyzed in this study.

**Conflicts of Interest:** The authors declare no conflicts of interest.

## References

1. Habib, M.A.; Hossain, M.J. Smart Grid, Smart FiT: A data-driven approach to optimize microgrid energy market. *Energy Policy* **2025**, *203*, 114618. [[CrossRef](#)]
2. Pramila, V.; Kannadasan, R.; Rameshkumar, T.; Rameshkumar, T.; Alsharif, M.H.; Kim, M.-K. Smart grid management: Integrating hybrid intelligent algorithms for microgrid energy optimization. *Energy Rep.* **2024**, *12*, 2997–3019. [[CrossRef](#)]
3. Pramila, V.; Rudhra, S.; Vinod, S.; Satish kumar, S.; Lakshmi, D. Enhancing demand response and energy management in multi-microgrid systems with renewable energy sources. *Renew. Energy* **2025**, *253*, 123490.
4. Kumari, S.; Chatterjee, K. Study the impact of renewable and non-renewable energy sources on micro-grid using time series data based information transfer. *Energy Rep.* **2024**, *11*, 4957–4966.
5. Tripathi, S.; Shrivastava, A.; Jana, K.C. An efficient energy management system for a micro-grid system considering the volatility of hybrid renewable energy. *Int. J. Hydrogen Energy* **2025**, *101*, 673–691. [[CrossRef](#)]
6. Liu, X.; Li, M.; Wang, R.; Feng, J.; Dong, C.; Sun, Q. Low-carbon operation of multi-virtual power plants with hydrogen doping and load aggregator based on bilateral cooperative game. *Energy* **2024**, *309*, 132984. [[CrossRef](#)]
7. Li, M.; Liu, X.; Li, J.; Yu, M.; Wang, R.; Sun, Q. A Bargaining Mechanism and Consensus Distributed Solving Method for P2P Trading among Prosumers Considering the Characteristics of Both Participants. *Sustain. Energy Grids Netw.* **2025**, *43*, 101778. [[CrossRef](#)]
8. Mobtahej, M.; Barzegaran, M.; Esapour, K. A novel Three-Stage demand side management framework for stochastic energy scheduling of renewable microgrids. *Sol. Energy* **2023**, *256*, 32–43. [[CrossRef](#)]
9. Guo, F.; Lian, Z.; Zheng, X.; Deng, C.; Wen, C.; He, J. Decentralized cluster-based distributed secondary control of large-scale DC microgrid cluster system. *IEEE Trans. Sustain. Energy* **2024**, *15*, 1652–1662. [[CrossRef](#)]
10. Armghan, H.; Xu, Y.; Bai, X.; Ali, N.; Chang, X.; Xue, Y. A tri-level control framework for carbon-aware multi-energy microgrid cluster considering shared hydrogen energy storage. *Appl. Energy* **2024**, *373*, 123962. [[CrossRef](#)]
11. Suo, Z.; Shi, H.T.; Meng, X.; Zhang, B.; Lan, L. A hierarchical evaluation method for power quality of microgrid cluster based on multi-temporal and spatial scales fusion analysis. *Electr. Power Syst. Res.* **2025**, *243*, 111473. [[CrossRef](#)]
12. Chen, Y.; Chakraborty, S.; Zamzam, A.; Wang, J. End-to-end microgrid protection using distributed data-driven methods. *Appl. Energy* **2025**, *391*, 125797. [[CrossRef](#)]
13. Sezgin, M.E.; Gol, M. Distributed energy management and communication strategy for network of microgrids. *Electr. Power Syst. Res.* **2025**, *238*, 111079. [[CrossRef](#)]
14. Chen, H.; Yang, S.; Wu, H.; Song, J.; Shui, S. Advanced hierarchical energy optimization strategy for integrated electricity-heat-ammonia microgrid clusters in distribution network. *Int. J. Hydrogen Energy* **2025**, *97*, 1481–1497. [[CrossRef](#)]
15. Tan, M.; Zhao, J.; Liu, X.; Su, Y.; Wang, L.; Wang, R.; Dai, Z. Federated Reinforcement Learning for smart and privacy-preserving energy management of residential microgrids clusters. *Eng. Appl. Artif. Intell.* **2025**, *139*, 109579. [[CrossRef](#)]

16. Ordoñez, J.G.; Barco-Jiménez, J.; Pantoja, A.; Revelo-Fuelagán, J.; Candelo-Becerra, J.E. Comprehensive analysis of MPC-based energy management strategies for isolated microgrids empowered by storage units and renewable energy sources. *J. Energy Storage* **2024**, *94*, 112127. [[CrossRef](#)]
17. Wang, B.; Ding, L.; Xiao, T.; Chen, Y. An integrated multi-timescale MPC framework for coordinated wind farm power maximization, load management, and grid support. *Renew. Energy* **2025**, *256*, 123903. [[CrossRef](#)]
18. Quan, X.; Wu, Z.; Xie, X.; Zeng, F.; Miu, H.; Yuan, X. Optimizing AC/DC microgrid scheduling with electro-hydrogen hybrid energy storage for low-carbon buildings. *Int. J. Hydrogen Energy* **2025**, *143*, 716–727.
19. Omrani, P.; Yektamoghadam, H.; Nikoofard, A.; Salehizadeh, M.R.; Liu, J.J. Dynamic congestion management with chance-constrained mpc in networked microgrids under consumers-related uncertainties. *IEEE Trans. Consum. Electron.* **2024**, *70*, 6738–6746. [[CrossRef](#)]
20. Pajares, A.; Vivas, F.J.; Blasco, X.; Herrero, J.M.; Segura, F.; Andújar, J.M. Methodology for energy management strategies design based on predictive control techniques for smart grids. *Appl. Energy* **2023**, *351*, 121809. [[CrossRef](#)]
21. Abdelghany, M.B.; Al-Durra, A.; Zeineldin, H.; Hu, J. Integration of cascaded coordinated rolling horizon control for output power smoothing in islanded wind–solar microgrid with multiple hydrogen storage tanks. *Energy* **2024**, *291*, 130442. [[CrossRef](#)]
22. Zhao, Z.; Xu, J.; Lei, Y.; Liu, C.; Shi, X.; Lai, L.L. Robust dynamic dispatch strategy for multi-uncertainties integrated energy microgrids based on enhanced hierarchical model predictive control. *Appl. Energy* **2025**, *381*, 125141. [[CrossRef](#)]
23. Vásquez, L.O.P.; Redondo, J.L.; Hervás, J.D.Á.; Ramírez, V.M.; Torres, J.L. Balancing CO<sub>2</sub> emissions and economic cost in a microgrid through an energy management system using MPC and multi-objective optimization. *Appl. Energy* **2023**, *347*, 120998. [[CrossRef](#)]
24. Luo, J.; Panchabikesan, K.; Lai, K.; Olawumi, T.O.; Mewomo, M.C.; Liu, Z. Game-theoretic optimization strategy for maximizing profits to both end-users and suppliers in building rooftop PV-based microgrids. *Energy* **2024**, *313*, 133715. [[CrossRef](#)]
25. Yang, M.; Wang, J.; Cao, X.; Gu, D. Economic dispatch of microgrid generation-load-storage based on dynamic bi-level game of multiple stakeholders. *Energy* **2024**, *313*, 133931. [[CrossRef](#)]
26. Wang, C.; Liu, Y.; Zhang, Y.; Xi, L.; Yang, N.; Zhao, Z.; Lai, C.S.; Lai, L.L. Strategy for optimizing the bidirectional time-of-use electricity price in multi-microgrids coupled with multilevel games. *Energy* **2025**, *323*, 135731. [[CrossRef](#)]
27. Wang, Y.; Cui, Y.; Li, Y.; Xu, Y. Collaborative optimization of multi-microgrids system with shared energy storage based on multi-agent stochastic game and reinforcement learning. *Energy* **2023**, *280*, 128182. [[CrossRef](#)]
28. Li, P.; Chen, J.; Yang, H.; Lin, Z. Peer-to-peer power trading and pricing for rental energy storage shared community microgrid: A coordinated Stackelberg and cooperative game. *Renew. Energy* **2025**, *256*, 123963. [[CrossRef](#)]
29. Qiao, J.; Mi, Y.; Shen, J.; Lu, C.; Cai, P.; Ma, S.; Wang, P. Optimization schedule strategy of active distribution network based on microgrid group and shared energy storage. *Appl. Energy* **2025**, *377*, 124681. [[CrossRef](#)]
30. Mohseni, S.; Pishvaei, M.S. Energy trading and scheduling in networked microgrids using fuzzy bargaining game theory and distributionally robust optimization. *Appl. Energy* **2023**, *350*, 121748. [[CrossRef](#)]
31. Cui, Z.; Chang, X.; Xue, Y.; Yi, Z.; Li, Z.; Sun, H. Distributed peer-to-peer electricity-heat-carbon trading for multi-energy virtual power plants considering copula-CVaR theory and trading preference. *Int. J. Electr. Power Energy Syst.* **2024**, *162*, 110231. [[CrossRef](#)]

**Disclaimer/Publisher’s Note:** The statements, opinions and data contained in all publications are solely those of the individual author(s) and contributor(s) and not of MDPI and/or the editor(s). MDPI and/or the editor(s) disclaim responsibility for any injury to people or property resulting from any ideas, methods, instructions or products referred to in the content.